Observation of Fretting Fatigue Cracks by Micro Computed Tomography with Synchrotron Radiation

D. Shiozawa[1], Y. Nakai[1], T. Kurimura[2] and K. Kajiwara[3]
[1]*Kobe University, Kobe, Japan;* [2]*Takasago Research & Development Center , Mitsubishi Heavy Industries, Hyogo, Japan,* [3]*Japan Synchrotron Radiation Institute, Hyogo, Japan*

Abstract
In the present study, micro computed tomography (μCT) with synchrotron radiation (SR) of SPring-8 was applied to observe and evaluate the fretting fatigue crack propagation in a Ti alloy. The shape of fretting fatigue cracks and crack coalescence could be evaluated quantitatively. The shape of fatigue cracks obtained by SR-μCT imaging agreed well with the geometry of fracture surface obtained by the stereogram analysis of scanning electron microscopy. Transition of crack propagation mode inside specimen in fretting fatigue could be observed nondestructively.

1. Introduction

Fretting is a small amplitude oscillatory movement, which may occur between contacting surfaces those are subjected to vibration or cyclic stress. It occurs typically in shafts, bearings, riveted and bolted connections, steam and gas turbines, and many other engineering applications. Fretting fatigue may result in premature and dramatic failure of machine components. However, fatigue strength and crack propagation behavior under fretting condition are still not completely understood because of its complexity. Contact between parts may induce a complex stress state, which affect the crack nucleation conditions, and multi-cracking. Since the change of fatigue crack propagation mode occurs in fretting fatigue, it is difficult to understand the propagation and crack coalescence behavior under the surface by using a surface observation method, such as conventional microscopies. To predict the life of components, the modeling of fretting fatigue based on the information of three-dimensional crack propagation is necessary.

The authors have been applied micro computed tomography with synchrotron radiation (SR-μCT) of Spring-8 to the 3D measurement of inclusions and crack in steels [1-3]. In the present study, SR-μCT imaging was applied to the observation of fretting fatigue cracks, and then the applicability of SR- μCT imaging of the evaluation of the fracture mode transition, multi-cracking, and crack coalescence was examined.

2. Experimental method

2.1 Sample

Fretting fatigue set-up and geometry of the sample observed in SPring-8 were shown in Fig. 1 [4]. Ti-6Al-4V alloy was used for the specimen to observe fatigue crack. The contact pad was the same material as the specimen. A contact

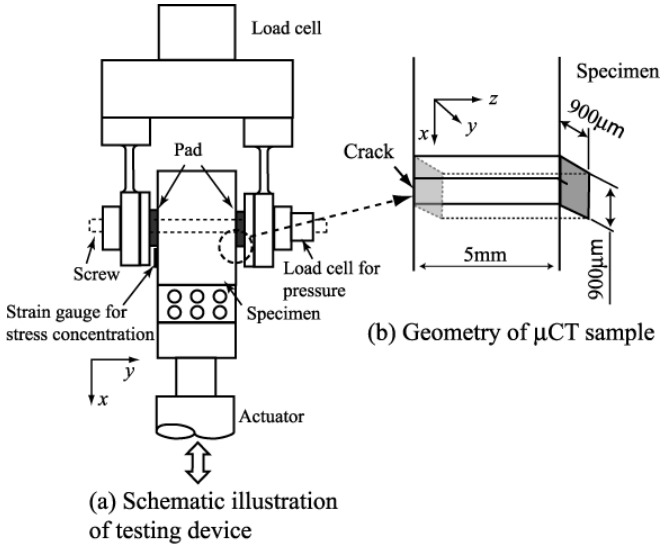

Fig. 1 Geometry of fretting fatigue set-up and sample

pressure of 98MPa was applied to the specimen through contact pads. The stress concentration at the edge of the contact pad on the specimen was measured by strain gauge. Constant amplitude cyclic loading with a stress ratio (R) of –1 and at a frequency of 20Hz was applied, where the nominal stress amplitude was 47.3MPa (bulk stress). The initial peak stress at the edge of contact pads was 300MPa. For Type A sample, fatigue tests were stopped when the output of strain gauge, which is glued near the contact edge, decreased by 20% from the initial value so that the fatigue cracks could be observed before final unstable failure. For Type B sample, to observe fatigue crack in earlier stage of fatigue, the fatigue tests were stopped when the output of the strain gauge decrease by 15% from the initial value. A part of the specimen near the contact edge, which includes cracks, was carved out from the specimen, and then they grinded until suitable size for obtaining projection images. In the previous X-ray imaging for stainless steel, samples for measuring small fatigue cracks, suitable size of the cross-section of sample was 300μm×300μm. Since the ratio of X-ray absorption coefficients of Fe to Ti is about 3, cross-section of the present sample was determined to be 900μm×900μm.

2.2 Measurement method

X-ray imaging was carried out at BL 19B2 beam line of SPring-8, which is the large synchrotron radiation facility in Japan. X-ray energy was adjusted to 35keV with silicon double-crystal monochromator. The distance between a bending magnet (X-ray source) and the specimen was about 100m. The projection image of penetrated X-ray was observed by an X-ray area detector. The detector was composed of a beam monitor (Hamamatsu Photonics AA50) and cooled CCD camera (Hamamatsu Photonics C4880 41S). Transmitted X-ray is converted to visible light through a thin phosphor screen and projected to the CCD camera by an optical relay-lens.

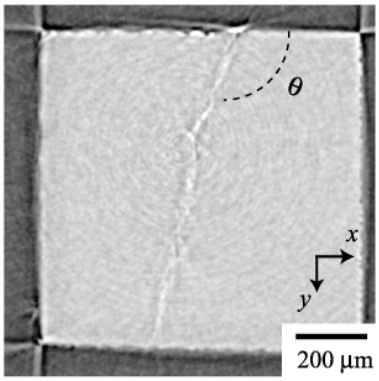

Fig. 2 Cross-sectional image by μCT
(at A-A' cross-section in Fig. 3(b))

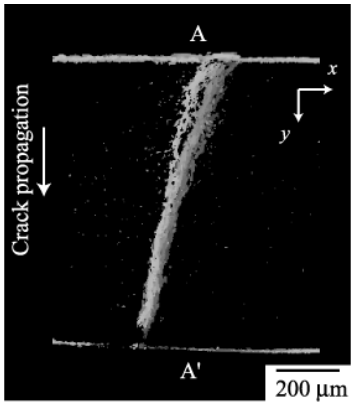

(a) 3D image (from View α)

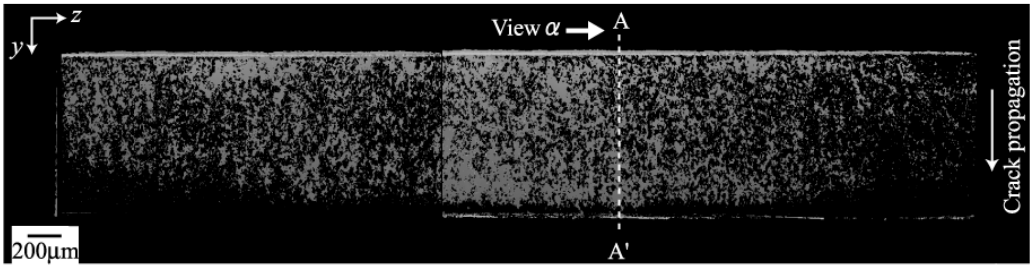

(b) 3D image by μCT

Fig. 3 3D image of fretting fatigue crack by SR-μCT

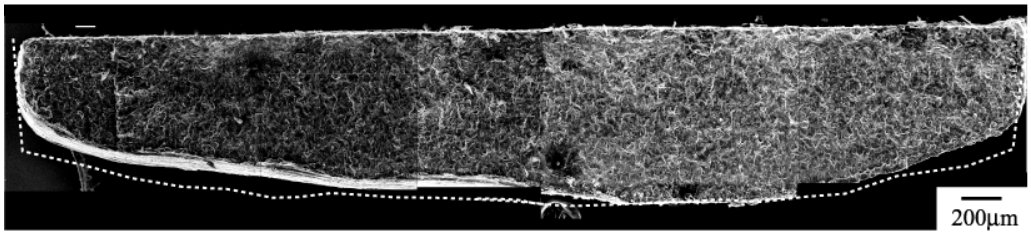

Fig. 4 SEM image of fracture surface

For Type A sample, a series of projection images of the specimen were obtained every 0.5° from 0° to 180° by rotating the specimen. To utilize the phase contrast effect, the X-ray area detector was set by 1.3m behind the sample. For Type B sample, images were obtained every 0.2° from 0° to 180°, and the distance between the sample and the detector was 0.8m. Slice images were reconstructed from the series of projection images by filtered-back projection algorithm.

3. Results

3.1 Type A sample

Fretting fatigue crack images were successfully obtained by SR-μCT imaging for Ti-alloy as shown in Fig. 2. This image indicates the map of X-ray absorption coefficient, and distinct white and black fringes might correspond to the opening cracks. Depending on the phase contrast effect and crack opening distance, cracks are obtained as white lines, black lines or both lines, since the phase contrast effect generates distinct white and black lines at interfaces of structure.

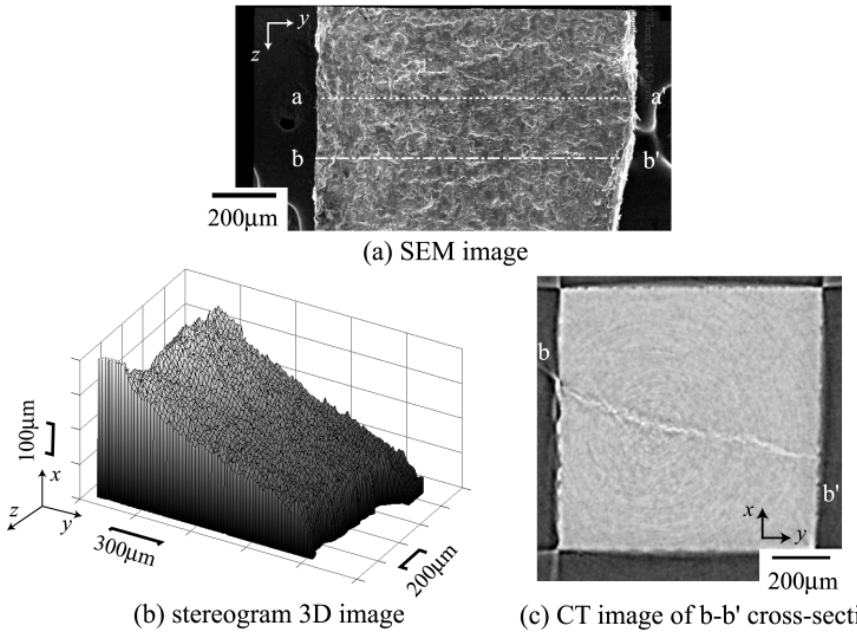

Fig. 5 Fracture surface observed by SEM, Stereogram analysis and SR--μCT

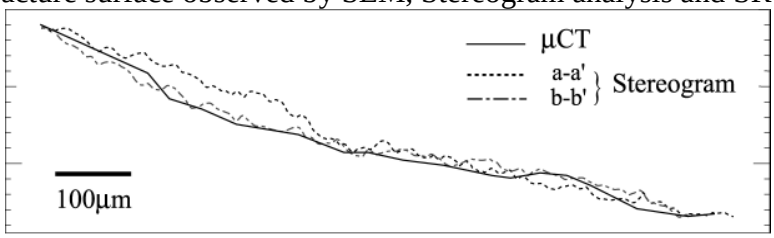

Fig. 6 Geometry of fracture surface

In Fig. 2, crack opening distance is small, so that the effect of absorption contrast is smaller than that of phase contrast. In order to emphasize the shape and the size of the crack, the μCT image was binarized, and black and white switched (negative image). The binarized 3D images are shown in Fig. 3. Figure 3(a) shows 3D image of the fatigue crack viewed from the direction of *z*-axis. The fretting fatigue cracks initiated and propagated at an angle θ from 110° to 120°, and the angle of the crack surface changed close to the *y*-direction as the crack grows. And then, the cracks had propagated at an angle of 95~100° at more than from 250 to 300μm in depth. The crack shows the typical fretting fatigue crack shape, which is divided into four stages: Stage I corresponding to the nucleation of a micro defect under the influence of the contact loads, Stage II is the inclined propagation of this defect into meso crack under the influence of the contact and bulk loads, Stage III is the propagation of the crack primarily under the influence of the bulk loads by tension mode (Mode I), and Stage IV is the final unstable failure of the specimen [5, 6].

Figure 3(b) shows the μCT image of the crack, which is viewed from the direction of *y*-axis in the specimen. The shape of the fretting fatigue crack is semi-elliptical, and the crack depth at the center is larger than that at the surface. To open the

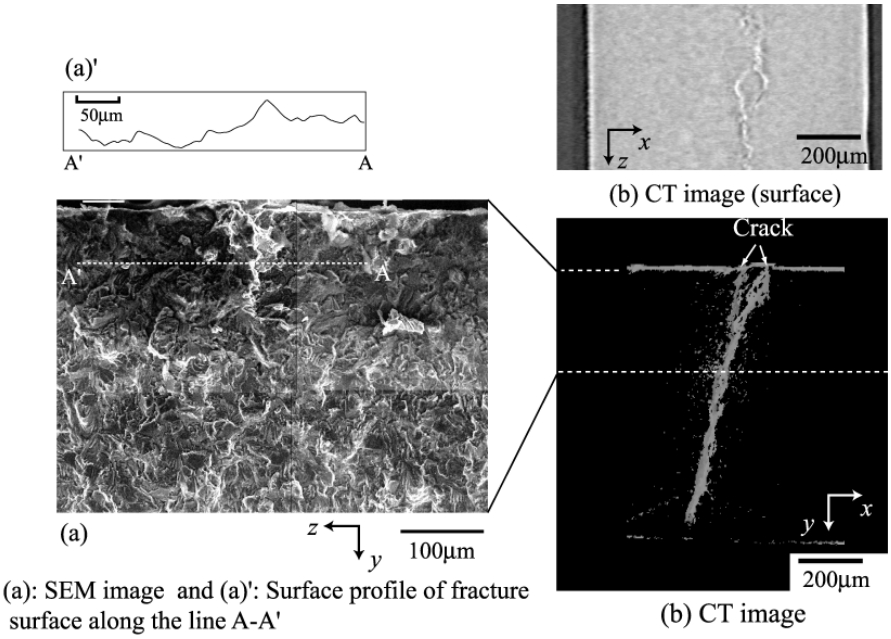

Fig. 7 Crack coalescence observed by SEM and SR-μCT

fracture surface for observation by SEM (scanning electric microscope), the ligament was grinded. Before the grinding, the shape of the crack was estimated from the crack shape obtained by the SR-μCT image. Figure 4 shows SEM image of fracture surface. In Fig. 4, the white dot line indicates the shape of crack estimated by SR-μCT image. The actual shape of crack opening agrees well with that observed by the SR-μCT image.

To evaluate the angle and the roughness of the fracture surface, stereogram analysis was carried with 3D image reconstruction software, MeX (Alicona inc.). Figure 5(a) and (b) shows SEM image of fracture surface and stereogram 3D image reconstructed from two SEM images, respectively. The stereogram was obtained by tilting ±3° from the top. The inclined fracture surface is also observed by the stereogram. Figure 5(c) shows the slice image by SR-μCT imaging at b-b' cross-section in Fig. 5(a). The geometry of fracture surface on the a-a' and b-b' dot line in Fig. 5(a) was plotted in Fig. 6. The crack shape obtained by SR-μCT imaging in Fig. 5(c) is also plotted in Fig. 6. The geometry of fracture surface by SR-μCT imaging agrees well with that by the stereogram analysis. It is found from Figs. 3(a) and 6 that the inclinations of the fracture surface decrease with increasing the depth, and the inclinations at more than 300μm in depth are almost same for any cross-sections. This change in inclination of fatigue crack is due to the influence of the contact loads, and the transition from Stage II to Stage III occurs from 250 to 300μm in depth.

Figure 7 shows crack coalescence in Type A sample. The step in the fracture surface is observed in SEM image and surface profile along A-A' (Fig. 7(a), (a)'). The step is located about 200μm below the surface, and the roughness of the fracture surface within 200μm in depth is smooth. At this step, the coalescence of

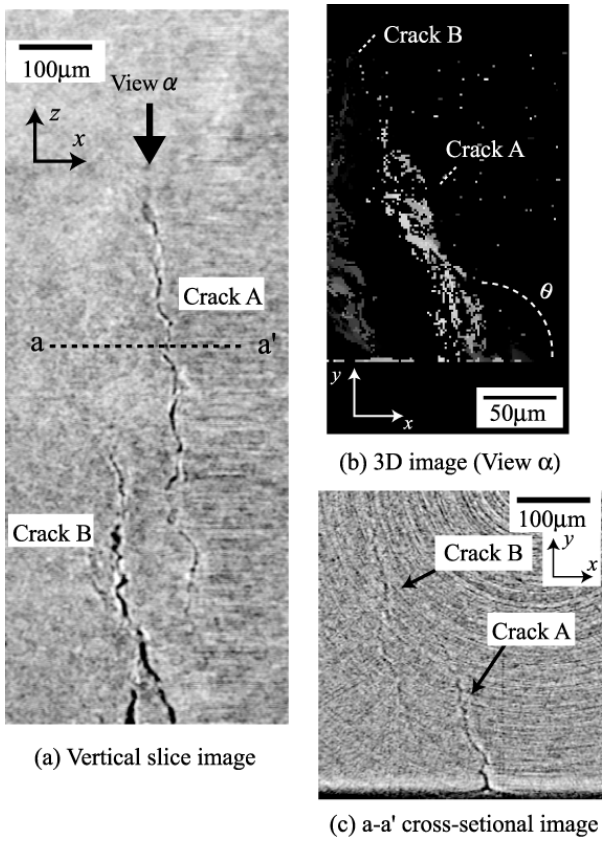

Fig. 8 SR-μCT images of fatigue cracks in Type B sample

two cracks is observed in the specimen as shown in Fig. 7(b). These two fatigue cracks merged each other at 200μm in depth, and then it grow as a single crack as shown in Fig. 7(c). These cracks are considered to have coalesced at the depth of transition of the stages, i.e., the fracture mode transition. SR-μCT imaging can nondestructively provide us the 3D information of crack coalescence, such as a location and depth.

3.2 Type B sample

To observe the early stage of fretting fatigue, the fatigue tests for Type B sample were stopped at earlier than that for Type A sample. Figure 8(a) shows the cross-sectional image (parallel to the surface) of Type B sample. Figure 8(b) shows reconstructed 3D image viewed from View α in Fig. 8(a). Crack A propagated at the angle of 115~120° and then inclination angle of Crack A keep constant independent of the crack depth. Crack A might be in Stage II of fretting fatigue. Crack B does not merged to Crack A. Figure 8(c) shows the slice image at a-a' dot line in Fig. 8(a). Crack B can not be observed on the surface (Fig. 8(a)), while it appeared in Fig. 8(c). It is considered that the tip of Crack B have propagated without crack opening on the surface due to the influence of contact loads.

Other cross-sectional images are shown in Fig. 9. Figure 9(a) shows many cracks parallel to Crack B, such as Crack C, D, and E. Figure 9(b) shows the

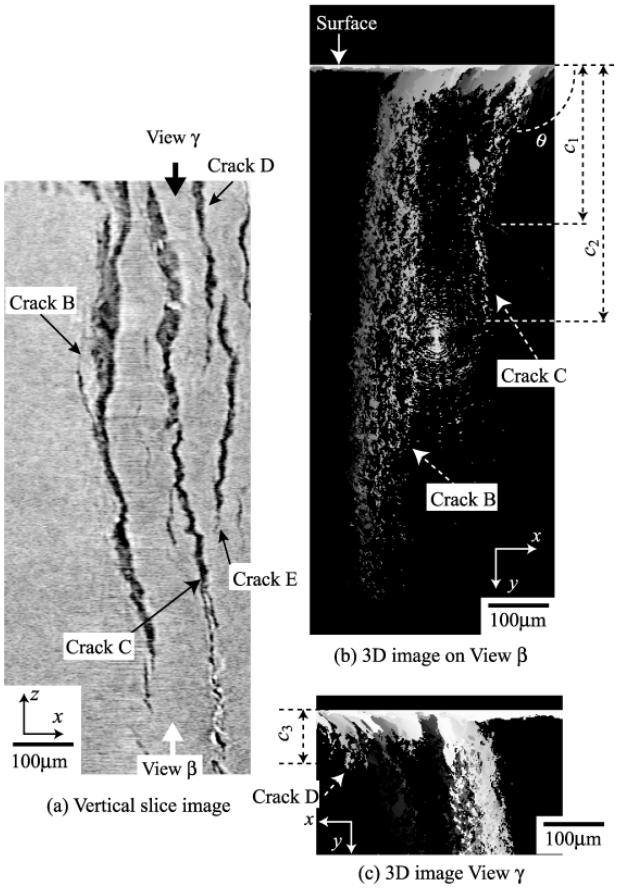

Fig. 9 SR-μCT images of small cracks in Type B sample

reconstructed 3D image viewed from View β. Crack C propagated to 220μm from the surface (c_1) at the angle of 115~120°. And then it propagated to the direction of *y*-axis. The propagation of Crack B is similar to that of Crack C and cracks in Type A sample. Figure 9(c) shows the 3D image near the surface viewed from View γ. Many small cracks, such as Crack D, and E, initiated at the angle from120° to 130°, and their depths are below 100μm. These cracks did not merge each other. They might to be in Stage I or early Stage II, and their behavior must be affected by the contact loads. Detail observation of these small cracks could not be accomplished by the SEM fractography.

Fatigue cracks in Stage I, II and III could be observed in Type B sample. The parallel cracks, such as Crack C, D, and E, could not be evaluated by the SEM fractography. Nondestructive method using SR-μCT imaging is useful to evaluate the behavior of multiple cracks and the coalescence of small cracks.

4. Conclusions

Imagings to evaluate the fretting fatigue crack propagation in Ti alloy were performed by μCT with synchrotron radiation of SPring-8. The results obtained are as follows:

(1) The shapes of fretting fatigue crack obtained by the SR-μCT imaging agreed well with the geometry of fracture surface obtained by SEM observation with stereogram analysis. The SR-μCT imaging could nondestructively evaluate the fretting fatigue crack propagation behavior.

(2) The transition of stage in fretting fatigue life in Ti alloy could be evaluated. The change in inclination of fatigue crack was observed inside. The transition from Stage II to Stage III occurred from 250 to 300μm in depth for this experiments.

(3) The coalescence of cracks could be nondestructively evaluated by using the SR-μCT imaging. At the present observation, however, no coalescence for cracks in Stage I or early Stage II was not be observed.

(4) Parallel multiple cracks and the distributions of these small cracks could be observed. For investigating parallel cracks, SEM fractography needs separation of specimen and provides the fragmentary information obtained from cross-sectional image, while nondestructive SR-μCT method provides useful information about subsurface cracks.

Acknowledgements
The synchrotron radiation experiments were performed at BL19B2 in SPring-8 with the approval of the Japan Synchrotron Radiation Research Institute (JASRI). Proposal numbers are 2007A1905 and 2007B1943.

References

[1] D. Shiozawa, Y. Nakai, Y. Morikage, H. Tanaka, H. Okado, ,and T. Miyashita, Qantitative Analysis of Inclusions in High-strength Steels by X-ray Computed Tomography Using Ultra-bright Synchrotron Radiation, Transactions of Japanese Society of Mechanical Engineers, Series A, Vol. 72, (2006) 1846-1852.

[2] D. Shiozawa, N. Nakai, T. Kurimura, Y. Morikage, H. Tanaka, H. Okado, T. Miyashita, K. Kajiwara, Observation of Cracks in Steels Using Synchrotron Radiation X-ray Micro Tomography, Journal of the Society of Materials Sciencem, Japan, Vol. 56, No. 10, (2007) 951-957.

[3] Y. Nakai, D. Shiozawa, Y. Morinaga, T. Kurimura, H. Okado, T. Miyashita, Observation of Inclusions and Defects in Steels by Micro Computed-tomography using Ultrabright Synchrotron Radiation, Fourth Int. Conf. on Very High Cycle Fatigue, J. E. Allison, J. W. Jones, J. M. Larsen, and R. O. Ritchie (Eds.), (2007), 67-72.

[4] Y.Kondo and M.Bodai, Based on Local Stress at Contact Edge, Transactions of Japanese Society of Mechanical Engineers, Series A, Vol.63, (1977) 669-676.

[5] Y. Mutoh, Fracture Mechanisms of Fretting Fatigue, Journal of the Society of Materials Sciencem, Japan, Vol. 46, No11, (1997) 1233-1241.

[6] L. Chambon, B. Journet, Modelling of Fretting Fatigue in a Fracture Mechanics Framework, Tribology International, 39, (2006), 1220-1226.